far upstream of the bowshock, streaming predominantly away from the Sun[6,7]. The fluxes measured by EPONA at Grigg-Skjellerup were almost a factor of 100 lower than those at Halley[7]. However, the particle energies at all three comets were similar ($\geqslant$ 260 keV) and always significantly exceeded the maximum energy attainable by the pick-up process alone.

The energetic particle profiles recorded at Grigg-Skjellerup were markedly different from those detected during previous encounters. In particular, the variations in fluxes at the oxygen ion cyclotron frequency recorded close to the nucleus have not been seen before. □

Received 2 October 1992; accepted 6 April 1993.

1. *Comets in the Post-Halley Era* (eds Newburn, R. L. Jr, Neugebauer, M. & Rahe, J.) (Kluwer, Dordrecht, 1991).
2. McKenna Lawlor S. *et al. J. Phys. E. Scient. Instrum.* **200**, 732–740 (1987).
3. Ip, W. H. & Axford, W. I. *Planet. Space Sci.* **34**, 1061–1065 (1986).
4. Neubauer, F. M. *et al. Astr. Astrophys.* **261**, L5–L8 (1993).
5. Coates, A. J. *et al. Geophys. Res. Lett.* **20**, 483–486 (1993).
6. Hynds, R. J. *et al. Science* **232**, 361–365 (1986).
7. McKenna-Lawlor, S. M. P. *et al. Icarus* **87**, 430–439 (1990).

Detection of the hydroxyl radical in the Saturn magnetosphere

D.E. Shemansky, P. Matheson, D.T. Hall*, H.-Y. Hu & T.M. Tripp†

Department of Aerospace Engineering, University of Southern California, Los Angeles, California 90089-1191, USA
* Department of Physics, Johns Hopkins University, Baltimore, Maryland 21218, USA
† Department of Astronomy, University of Wisconsin, Madison, Wisconsin 53706, USA

THE magnetosphere in the vicinity of the orbits of Saturn's icy satellites consists of a low-density plasma, in which the electrons are an order of magnitude cooler than the accompanying heavy ions[1]. Most models[2–12] neglect this fact, even though radiative cooling and diffusive loss rates are both too slow to account for the observed temperatures. Shemansky and Hall[13] have recently proposed that the electrons could be cooled by the presence of a large abundance of neutral gas, derived mainly from the breakdown products of H_2O (mainly O and OH) from the icy satellites. Hydrogen radicals have been reported in this region[13], but these originate from the atmosphere of Saturn itself; no satellite-derived neutral species have been detected. Here we report the detection of neutral OH molecules near the orbit of Tethys, using the Faint Object Spectrograph on the Hubble Space Telescope. Our results suggest that neutral OH is one of the dominant species in Saturn's inner magnetosphere, implying a source rate for H_2O twenty times greater than current theoretical estimates[5,6]. One possible explanation is that the micrometeorite erosion rates of the inner satellites are significantly higher than expected.

Spectra of Saturn's magnetosphere were obtained in two sets of exposures on 24 and 26 August 1992. The observations were made from the dark Earth atmosphere, along a line of sight passing through the satellite plane and displaced by 4.5 Saturn radii (R_S) from the centre of Saturn on the local dusk side. This location coincides with a maximum in the abundance of magnetosphere plasma, as modelled[1] from Voyager spacecraft observations, and was expected to correspond to a maximum in neutral gas abundance[13]. The gas was assumed to be in stable orbit around the planet, and the dusk side of the planet was selected for observation because positive heliocentric radial velocities (that is, velocities away from the Sun) provide a maximum scattering efficiency for solar radiation. The scattering of solar radiation is expected to be the chief emission process in this case, just as it is in comet atmospheres. The line of sight was clear of satellites, so could be acquired entirely from the magnetospheric gas. A spectrograph aperture was selected for maximum throughput limited by a desired wavelength resolution ($\lambda/\Delta\lambda$) of at least 600. The total exposure time for the two days of observations was about 3.5 hours. The dispersive dimension of the selected aperture was 4.4 Å. Other observational details are given in Fig. 1. The spectra obtained on the two days showed no detectable differences, and were combined to minimize signal noise. The calibrated spectrum was produced using the standard procedure of flat fielding and subtraction of sky background before calibration. Figure 1 shows the spectrum, which includes a substantial component following the shape of the solar spectrum. Such a component is expected because of sunlight scattered from the rings of Saturn, which were near maximum inclination and only 20 arcsec from the instrument's field of view. The signal in excess of the scattered solar spectrum near 3,085 Å is attributed to OH.

The solar spectrum has been accurately measured at high resolution[14] at wavelengths longer than 2,960 Å. This spectrum has been used to predict the spectrum of OH emission in radiative equilibrium. Models calculated on this basis have accurately matched comet spectra[15], and we have used our current code to match the spectrum obtained by the International Ultraviolet Explorer for comet Halley (T.M.T., D.E.S., D.T.H. and T.H.M., manuscript in preparation). Figure 1 shows the synthesized solar spectrum, scaled to match the observed spectrum in the wavelength intervals 3,000 – 3,030 Å and 3,120 – 3,150 Å. The difference spectrum plotted in Fig. 1 shows excess emission near 3,085 Å matched by the OH band emission model. The OH model combines solar and electron excitation processes in a statistically equilibrated system. Solar fluorescence dominates, and deleting the plasma excitation has negligible effect. The observed and synthesized spectra show a good match to the main feature, the A – X (0,0) band. Other possible features are at the noise level. The OH gas orbiting at 4.5 R_S has a bulk velocity vector of +10.4 km s^{-1} along the line between the Sun and the point of observation. The brightness of the OH (A $^2\Sigma+$ – X $^2\Pi$) (0,0) band determined from the model fit to the data is 37 ± 12 Rayleighs (R). Given the known solar flux[14] and the plasma parameters in Table 1, our calculated value for the excitation probability of the OH band is 4.1×10^{-6} s^{-1}. With the spatial parameters of ref. 13, this translates to a mean density of 160 ± 50 molecules cm^{-3}.

Table 1 compares observations and theoretical calculations relevant to the present results. We summarize previous observations of neutral gas here. Consideration of the physical chemistry of H_2O extracted from the icy satellites predicts the presence of H, O, OH and other products indicated in Table 1. The hydroxyl radical has not previously been observed. Atomic hydrogen was first detected in 1975[16] and confirmed by later observations. It was generally assumed that the hydrogen was an escape product from the Titan atmosphere. The lack of spatial resolution in the earlier measurements did not allow confirmation of the location of the source. Observations obtained by the Voyager Ultraviolet Spectrograph System (UVS) provides better spatial definition, but the first reported results[17] were based on a limited subset of the data. The distribution was described as a torus with an inner radius of ~ 8 R_S, the inner region being essentially devoid of neutral gas (see Table 1). Shemansky and Hall[13], in an extensive analysis of the Voyager UVS data, discount this result, and claim that the inner magnetosphere in fact contains most of the gas in the system, with increasing densities of H merging into the planet atmosphere. The initial description[17] is, according to the analysis of

TABLE 1 Observed and modelled magnetosphere populations

Observations at ~ 5 R_S	Date	Method	[H]	[OH]	[H†]	[O^+(OH^+)]	Comment
Broadfoot *et al.*[17]	1981	Voy UVS*	0				'H'-cavity†
Richardson and Sittler[1]	1981	Voy PLS‡			2.8	29	Peak values
Shemansky and Hall[13]	1981	Voy UVS§	100				increases inward
Current	1992	HST-FOS‖		160			
Models	$\dot{N}_{H_2O}$	$\dot{N}_H$	[H]	[O(OH)]	[H†]	[O^+(OH^+)]	Transport time (days)
Eviatar[4]	1¶						~ 900
Richardson *et al.*[7]#	1	0.23	6.1	2.2 (2.4)	2.1	3.4 (1.9)	∞
Richardson and Eviatar[8]	1**	~ 0.4	8	9	2.5	9.5	∞
Richardson and Eviatar[9]	1††	1††			3	15‡‡	∞
Johnson *et al.*[5]§§	0.7	1		~ 5	~ 2	~ 25	
Barbosa[10]	1	10	6			~ 25‖‖	30
Shemansky and Hall[13]	28	0	136	414 (35.5) ¶¶	3.29	24.5 (1.05)	40
Richardson[12]	1.0		5		~ 2 §§	~ 25 §§	5,400
Current##	24.8	12.6***	100	199 (160)	3.15	19.5 (4.51)	30

All local densities are in cm^{-3}. [O^+(OH†)] and [O(OH)] represent total heavy component unless both O and OH and/or O^+ and OH^+ are specified. $\dot{N}_{H_2O}$ is the total heavy neutral source ($\times 10^{26}$ s^{-1}) and N_H the total hydrogen source ($\times 10^{26}$ s^{-1}).

* Summed scans of H Ly-α. Poor coverage of inner region.

† We consider this result to be erroneous.

‡ Voyager Plasma Science Experiment; heavy ion components from water are mutually indistinguishable.

§ Reanalysis of Voyager H Ly-α scans. Complete coverage of area.

‖ Source brightness of 37R in OH 3,085 Å band.

¶ Ring source. Only 10^{24} s^{-1} ions produced in Dione–Tethys Region.

\# Results of model calculations at 5 eV.

** Inferred rate.

†† Inferred from model's timescale, Fig. 8.

‡‡ Heavy ion is assumed to be H_2O^+.

§§ Approximate average equatorial values shown. Ion data are from PLS model.

‖‖ Inferred from Fig. 4 of paper.

¶¶ OH photodissociation rate is 5.6 times too high.

\## Cold electron density and temperature [e_c] = 31.4 cm^{-3} and [T_{ec}] = 4 eV. Hot electron density and temperature [e_h] = 0.4 cm^{-3} and [T_{eh}] = 120 eV.

*** Implied rate. Calculation held [H] = 100 cm^{-3} fixed.

ref. 13, not supported by the reduced data set. The observed atomic hydrogen is latitudinally extensive[13,18] and longitudinally non-uniform[13], indicating that its source is Saturn's atmosphere[13]. Atomic hydrogen from the icy satellites has never been observationally identified, primarily because of masking by the source at Saturn. Atomic oxygen has not been detected, because it does not efficiently scatter solar radiation.

Theoretical calculations predicting the content of the inner magnetosphere are summarized in Table 1. Of these, only ref. 13 tolerates more than a very small population of neutral gas. Consequently, the idea of substantial amounts of H in the inner region has essentially been rejected[2-12,19]. The large abundance of OH reported here also runs counter to the reports summarized in Table 1, with the exception of ref. 13. In fact, the observed abundance of OH is larger than predicted in ref. 13. We find, however, that the rate coefficient for the photodissociation of OH used there was 5.6 times too high, and resulted in an underestimate for OH density. Corrected values appear in the last row of Table 1. This updated model predicts that atomic oxygen should be the dominant species.

The strong disagreement between the observations of substantial amounts of neutral gas and most published theories of the inner magnetosphere does not have a simple explanation and cannot be fully addressed here. In the principal theories[2-12] neutral gas abundance is limited by the restriction in the mass loading rate of the plasma, either through calculated limits on source rates at the icy satellites, or through assumed limitation on the diffusive loss of plasma from the system. In reality the large neutral abundance controls the loss of plasma through charge exchange. Most recent calculations[10,11,12,19] use a com-

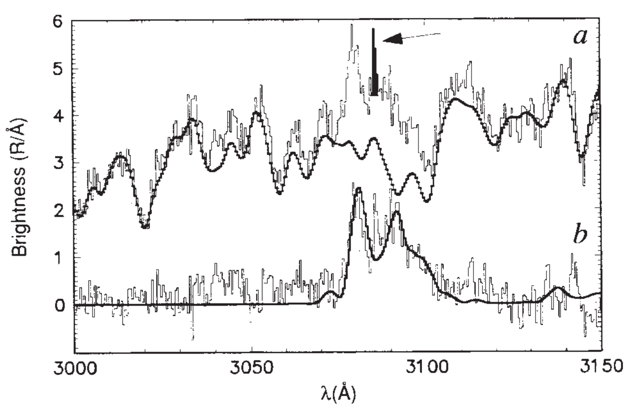

FIG. 1 *a*, Accumulated reduced FOS spectrum of ~ 3.5 hours integrated observation time, shown in the region of the OH A – X (0,0) band near 3,085 Å (light line). A solar model (heavy line) convolved with the instrument transmission function and scaled to the observation is superposed. Solar photons are scattered into the instrument from the nearby rings. Signal contamination from incomplete fixed pattern noise correction is indicated by the arrow. *b*, Difference spectrum along with an OH model spectrum (heavy line). The unambiguous presence of OH is manifest by the A – X (0,0) band emissions near 3,085 Å. No other features in the difference spectrum are identified above the noise level. The observations were obtained using the FOS red detector and G270 grating, which covers the approximate range 2,000 – 3,200 Å. A spectral resolution of 4.4 Å was achieved using the 0.7 × 2-bar (C-4) aperture. The telescope was pointed 4.5 R_S from Saturn's centre on the dusk side, to coincide with the observed maximum in plasma abundance. The exposures were obtained in the night sky on 24 and 26 August 1992. No satellites were in the field of view during the exposures. The data from each day were accumulated into the single reduced spectrum shown above. The source brightness in the OH band is 37 ± 12 rayleighs. Ordinate unit R/Å is in rayleighs per ångstrom.

mon limit on source rate established by the calculations of Pospieszalska and Johnson[6], although other differences exist between them. The source in this case is limited to the icy satellites. The ring system is excluded as a possible source because a prohibitively large average kinetic energy (25 eV per molecule) is required to deliver the H_2O to the orbital location of the observation. The model used in ref. 13, which resulted in the prediction of large neutral abundances of H_2O products, differed from the other works in two respects. First, source and diffusive loss characteristics were dictated by the measured plasma parameters such as ion partitioning. Second, an approximate balance in the energy budget was required as part of the calculation. It is argued that the measured temperature of the ambient electrons (~ 4 eV) can only be explained by the cooling mechanism provided by a relatively high density of neutral gas. The calculations of ref. 13 and the current correction of those results essentially agree with the observations (Table 1).

The total estimated source rates can be obtained from a volumetric partitioning code[13] (last entry, Table 1). The hydrogen number density is fixed at $[H] = 100\ cm^{-3}$ to correspond to the hydrogen abundance observed by Voyager 1. The source is considered to be a mix of water and oxygen, where the oxygen source represents a population of satellite gas formed from dissociation of water while still in the satellite's tenuous atmosphere, or near its surface. The total source rate is calculated for a total gas volume of 3×10^{31} cm^3, which corresponds to the annular volume defined by the orbits of the satellites Enceladus and Rhea and the region $\pm$ 0.25 R_S out of the equatorial plane. The calculation assumes a mass-dependent diffusive loss time in order to reduce the proton content to the value reported for the Voyager plasma[1]. The total source rate remains about 2×10^{27} s^{-1} as calculated by ref. 13, or about 20 times higher than those proposed by the other models. Large amounts of OH imply equally large amounts of neutral O. The partitioning of $[O^+]$, $[OH^+]$ and $[H_2O^+]$ varies with the relative source rates of O and H_2O.

The large source rate required by the observations may force us to reassess our understanding of Solar System structure. Water products in the magnetosphere have been assumed to be produced when magnetospheric plasma sputters H_2O molecules off the icy satellite surfaces. If this source is inadequate, a plausible explanation may be that primordial material in the form of micrometeorites contributes to the sputtering. The implication is that the flux of these particles is much larger than previously believed.

The measured abundances indicate that the local plasma electron temperature and hence rate processes in the system are determined by the quenching effect of the neutral gas[13]. This is in sharp contrast to the plasma conditions at Jupiter. A general expectation for an internally sustained plasma torus controlled by radiative loss is that it relaxes to a dominantly neutral gas[20]. However, the ratio of neutral number density of electron density ($[N]/[e]$) in the equatorial region of Saturn's magnetosphere near 4.5 R_S is of order 10, whereas in the Jovian Io plasma torus $[N]/[e] \approx 0.02$. This suggests that there are fundamental differences in energy source mechanisms for the two systems (see ref. 20), with Jupiter's plasma torus apparently requiring an external energy source. The large source rate of mass at Saturn indicates that it may be possible to observe OH in the Jupiter system, particularly near the orbit of Europa, where increased amounts of oxygen have been reported[21]. □

Received 4 December 1992; accepted 20 April 1993.

1. Richardson, J. D. & Sittler, E. C. *J. geophys. Res.* **95**, 12019–12031 (1990).
2. Ip, W. H. *Astrophys. J.* **246**, 344–353 (1981).
3. Sieveka, E. M. & Johnson, R.E. *Icarus*, **51**, 528–548 (1982).
4. Eviatar, A. *J. geophys. Res.* **89**, 3821–3828 (1984).
5. Johnson, R.E. *et al. Icarus* **77**, 311–329 (1989).
6. Pospieszalska, M. K. & Johnson, R.E. *Icarus* **93**, 45–52 (1991).
7. Richardson, J. D., Eviatar, A. & Siscoe, G. L. *J. geophys. Res.* **91**, 8749–8755 (1986).
8. Richardson, J. D. & Eviatar, A. *Geophys. Res. Lett.* **14**, 999–1002 (1987).
9. Richardson, J. D. & Eviatar, A. *J. geophys Res.* **93**, 7297–7306 (1988).
10. Barbosa, D. D. *J. geophys. Res.* **95**, 17167–17177 (1990).
11. Eviatar, A. & Richardson, J. D. *Ann. geophys.* **8**, 725–732 (1990).
12. Richardson, J. D. *J. geophys. Res.* **97**, 13705–13713 (1992).
13. Shemansky, D. E. & Hall, D. T. *J. geophys. Res.* **97**, 4143–4161 (1992).
14. Kurucz, R. L., Furenlid, I., Brault, J. & Testerman, L. *Solar Flux Atas for 296 to 1300 nm* (Harvard Univ. Press, 1984).
15. Schleicher, D. G. & A'Hearn, M. F. *Astrophys. J.* **331**, 1058–1077 (1988).
16. Weiser, H., Vitz, R. C. & Moos, H. W. *Science* **197**, 755–757 (1977).
17. Broadfoot, A. L. *et al. Science* **212**, 206–211 (1981).
18. Hilton, D. A. & Hunten, D. M. *Icarus* **73**, 248–268 (1988).
19. Eviatar A. & Richardson, J. D. *Ann. geophys.* **10**, 511–518 (1992).
20. Shemansky, D. E. *J. geophys. Res.* **93**, 1773–1784 (1988).
21. Bagenal, F., Shemansky, D. E., McNutt, R. L. Jr, Schreier, R. & Eviatar, A. *Geophys. Res. Lett.* **19**, 79–82 (1992).

ACKNOWLEDGEMENTS. This work is supported by grants from the Space Telescope Science Institute and the NASA Planetary Atmospheres Program.

Origin of luminescence from porous silicon deduced by synchrotron-light-induced optical luminescence

T. K. Sham, D. T. Jiang, I. Coulthard, J. W. Lorimer, X. H. Feng, K. H. Tan, S. P. Frigo*, R. A. Rosenberg†, D. C. Houghton‡ & B. Bryskiewicz‡

Department of Chemistry, The University of Western Ontario, London, Ontario N6A 5B7, Canada
*Synchrotron Radiation Center, University of Wisconsin-Madison, Stoughton, Wisconsin 53589, USA
†Advanced Photon Source, Argonne National Laboratory, Argonne, Illinois 60439, USA
‡Institute for Microstructural Science, National Research Council, Ottawa, Ontario K1A 0R6, Canada

FOLLOWING reports of intense optical luminescence from porous silicon[1,2], the opportunity for engineering optoelectronic devices using this material[3,4] has attracted considerable attention. At present, however, the question of the origin of the luminescence has not been fully resolved[5]. The quantum-confinement model[6–8] suggests that a quantum size effect gives optical transitions, and hence luminescence, in the visible range — this idea gains support from the wavelength dependence of the luminescence on porosity. An alternative model[9,10] attributes the luminescence to siloxene-like compounds[11] formed on the silicon surface. A third model, which invokes hydrogenated amorphous silicon as a possible source[12,13], seems to be contradicted by X-ray absorption fine structure (XAFS) studies[14–16]. Here we report optical luminescence in porous silicon and siloxene induced by soft X-rays with energies near the silicon K-edge (1,839 eV). Using the luminescence together with the total electron yield, we can obtain the XAFS spectra for the luminescent sites in both materials. Our results show that the luminescence from porous silicon does not derive from siloxene (either freshly prepared or annealed), and thus suggest that the quantum-confinement model seems to provide the only viable explanation.

Previous work on synchrotron-radiation-induced luminescence near an absorption threshold of a core level[18–24] has shown that the optical luminescence yield depends strongly on the site and chemical environment of the absorbing atom[18]. The potential of XAFS[19] to shed light on the structural and electronic properties of porous silicon has already been demonstrated[14–16]. Here we attempt to determine whether the luminescence can be ascribed to quantum confinement or to siloxene, using XAFS combined with X-ray excited optical luminescence (XEOL)[18,20–22] at the Si K-edge. The total optical photon yield is recorded as a function of soft X-ray energy across